AGU PUBLICATIONS

Geophysical Research Letters

RESEARCH LETTER
10.1002/2013GL058405

Key Points:
- Above-cloud aerosol optical depths derived from A-train sensors are compared
- Agreement between sensors is robust over homogeneous cloud fields
- CALIOP 532 nm retrieval was underestimated but its 1064 nm is in close agreement

Correspondence to:
Hiren Jethva,
hiren.t.jethva@nasa.gov

Citation:
Jethva, H., O. Torres, F. Waquet, D. Chand, and Y. Hu (2014), How do A-train sensors intercompare in the retrieval of above-cloud aerosol optical depth? A case study-based assessment, *Geophys. Res. Lett.*, *41*, 186–192, doi:10.1002/2013GL058405.

Received 21 OCT 2013
Accepted 15 DEC 2013
Accepted article online 18 DEC 2013
Published online 15 JAN 2014

How do A-train sensors intercompare in the retrieval of above-cloud aerosol optical depth? A case study-based assessment

Hiren Jethva[1,2], Omar Torres[2], Fabien Waquet[3], Duli Chand[4], and Yongxiang Hu[5]

[1]Universities Space Research Association, Columbia, Maryland, USA, [2]NASA Goddard Space Flight Center, Greenbelt, Maryland, USA, [3]Laboratoire d'Optique Atmospherique, Universite Lille, Villeneuve d'Ascq, France, [4]Pacific Northwest National Laboratory, Richland, Washington, USA, [5]NASA Langley Research Center, Hampton, Virginia, USA

Abstract We intercompare the above-cloud aerosol optical depth (ACAOD) of biomass burning plumes retrieved from A-train sensors, i.e., Moderate Resolution Imaging Spectroradiometer (MODIS), Cloud-Aerosol Lidar with Orthogonal Polarization (CALIOP), Polarization and Directionality of Earth Reflectances (POLDER), and Ozone Monitoring Instrument (OMI). These sensors have shown independent capabilities to retrieve aerosol loading above marine boundary layer clouds—a kind of situation often found over the southeast Atlantic Ocean during dry burning season. A systematic comparison reveals that all passive sensors and CALIOP-based research methods derive comparable ACAOD with differences mostly within 0.2 over homogeneous cloud fields. The 532 nm ACAOD retrieved by CALIOP operational algorithm is underestimated. The retrieved 1064 nm AOD however shows closer agreement with passive sensors. Given the different types of measurements processed with different algorithms, the reported close agreement between them is encouraging. Due to unavailability of direct measurements above cloud, the validation of satellite-based ACAOD remains an open challenge. The intersatellite comparison however can be useful for the relative evaluation and consistency check.

1. Introduction

Atmospheric aerosols in cloud-free scenes generally produce a net negative radiative effect (cooling) at the top-of-atmosphere (TOA). However, elevated layers of absorbing aerosols above cloud can potentially exert a significant level of atmospheric absorption and produce a positive radiative forcing at TOA [*Keil and Haywood*, 2003; *Chand et al*., 2009]. The magnitudes of the forcing directly depend on the microphysical and optical properties of the aerosol layer and underlying cloud. Conventional satellite retrievals of aerosols are restricted to the cloud-free regions, which severely limits our understanding of the aerosol effects on cloud radiative forcing and microphysical properties.

There has been a growing interest in the recent years on quantifying the aerosol loading above cloud from satellite-based active as well as passive measurements. Several algorithms have been introduced by different research groups employing different types of satellite measurements to retrieve the above-cloud aerosol (ACA) optical depth (ACAOD). The Cloud-Aerosol Lidar with Orthogonal Polarization (CALIOP) sensor employs an operational aerosol algorithm that uses estimated vertical extinction profile derived from the backscatter measurements and assumed lidar ratio (extinction to backscatter) to derive the AOD in clear as well as cloudy skies [*Winker et al*., 2009; *Young and Vaughan*, 2009]. Alternative CALIOP-based research methods, namely, the depolarization ratio (DR) [*Hu et al*., 2007] and the color ratio (CR) [*Chand et al*., 2008], respectively, have also been introduced to retrieve ACAOD. *Waquet et al*. [2009] make use of polarized radiances measured by the Polarization and Directionality of Earth Reflectances (POLDER) to retrieve AOD above cloud. An operational version of this algorithm has also been developed, which is capable of retrieving ACAOD globally [*Waquet et al*., 2013]. Taking the advantage of enhanced aerosol absorption sensitivity in the near-UV, *Torres et al*. [2012] introduced an innovative technique to retrieve ACAOD and underlying aerosol-corrected cloud optical depth (COD), simultaneously, from observations by the Ozone Monitoring Instrument (OMI). *Jethva et al*. [2013] have developed a color ratio method which employs one visible and one shortwave IR (SWIR) channel measurements from the Moderate Resolution Imaging Spectroradiometer (MODIS) to deduce a pair of ACAOD and aerosol-corrected COD, simultaneously.

Validation of the above-cloud AOD retrieval is a challenging task primarily due to lack of adequate direct measurements of aerosols above cloud. A few field campaigns such as Southern African Fire-Atmosphere Research Initiative 2000 [*Haywood et al*., 2004] and Tropospheric Aerosol Radiative Forcing Observation Experiment carried out aerosol measurements in the clear as well as cloudy atmosphere. However, these data sets have limited samplings in time and space and also not meant to measure the aerosols above cloud in particular. In this situation, an intercomparative analysis of the existing research retrievals from different sensors would be helpful to check the consistency (or lack thereof) among entirely independent techniques. In this paper, we intercompare the coincident research retrievals of ACAOD retrieved using six entirely independent techniques applied to four sensors, i.e., MODIS, CALIOP, POLDER, and OMI-flying in line formation in the A-train satellite constellation. Two events of biomass burning aerosols above cloud are selected over the southeast Atlantic Ocean (SEAO), where smoke aerosols generated from the intense biomass burning in central Africa are often transported westward over the oceanic low-level stratocumulus cloud deck. We emphasize here that the present study does not constitute the "validation" of the ACA retrieval, instead, the objective of this study is to check the consistency among entirely independent techniques that have been developed to measure the above-cloud aerosol loading. A brief description of the different ACA techniques and data set are given in section 2. The results of intercomparison are presented in section 3. Possible sources of uncertainties associated with each method are discussed in section 4.

2. A Brief Description of ACA Techniques and Data Sets

2.1. MODIS

The presence of absorbing aerosol layer above cloud reduces the TOA reflectance and CR between the visible and SWIR wavelengths. The general CR technique developed by *Jethva et al*. [2013] exploits this signal and uses reflectance at two channels, i.e., 470 nm and 860 nm to retrieve ACAOD and underlying COD, simultaneously. The method requires MODIS TOA reflectance (MYD021KM), geolocation data (MYD03), and MODIS cloud product (MYD06) for cloud screening all of them at 1 km resolution. These products were obtained from http://ladsweb.nascom.nasa.gov/data/. The aerosol model required to generate look-up-table (LUT) was based on the monthly statistics of Aerosol Robotic Network (AERONET) measurements at an inland site, Mongu (15°S, 23°E), Zambia, in southern Africa. The retrieved ACAOD at 860 nm was converted to 500 nm following the spectral extinction assumed in the aerosol model.

2.2. OMI

The near-UV technique applied to the OMI observations makes use of two-channel measurements (354 and 388 nm) to retrieve ACAOD and underneath COD, simultaneously. An increased sensitivity of TOA signal to the aerosol absorption above cloud in the near-UV region has been exploited to retrieve ACA, which, under a prescribed set of assumption, can be directly related to the magnitude of ACAOD and COD. The OMI TOA orbital data for the two case studies was obtained from NASA Goddard Earth Sciences Data and Information Services Center (GES-DISC) (http://disc.sci.gsfc.nasa.gov/Aura/data-holdings/OMI/omaeruv_v003.shtml). Aerosol microphysical properties assumed for LUT were acquired from the existing OMAERUV standard carbonaceous aerosol models. A full description of the algorithm is given by *Torres et al*. [2012]. The retrieved near-UV ACAOD at 388 nm was converted to 500 nm, assuming the model-based spectral extinction for the intersatellite comparison.

2.3. CALIOP

The operational CALIOP algorithm employs feature and layer detection scheme [*Winker et al*., 2009] combined with an extinction retrieval algorithm [*Young and Vaughan*, 2009] that requires an assumption on the extinction-to-backscatter ratio to retrieve the height-resolved extinction profile and columnar AOD at 532 nm and 1064 nm wavelengths at 5 km scale (level 2). The level 2 CALIOP data (V3.01) were obtained from NASA Langley's Atmospheric Science Data Center (ASDC) web portal (https://eosweb.larc.nasa.gov/project/calipso/cal_lid_l2_05kmalay-prov-v3-01_table).

In addition to the operational CALIOP method, two alternative active remote sensing techniques, namely, depolarization ratio and color ratio, have been developed to deduce ACAOD from CALIOP observations. These techniques are based on light transmission methods that use bright and commonly available lidar targets of liquid water clouds underneath the aerosol layers. These methods utilize three properties, i.e., layer integrated attenuated backscatter and depolarization ratio at 532 nm, and layer-integrated attenuated color

Table 1. Salient Properties of the ACA Retrieval Techniques and Associated Sensors

	Physical Basis	Algorithmic Assumptions	Input Parameters	Retrieved Parameters	Retrieval Uncertainty
MODIS *Jethva et al.* [2013]	Change in the reflectance and color ratio in the visible (VIS)/SWIR when absorbing aerosols overlay cloud	Aerosol/cloud size distribution, aerosol spectral extinction and absorption, aerosol/cloud profiles, and surface albedo	TOA reflectance at 470 and 860 nm at $1 \times 1\ km^2$ resolution	ACAOD and aerosol-corrected COD at 860 nm; converted to 500 nm based on the model assumed spectral extinction	Depends on ACAOD and COD. Typically between −12 and 46% at COD of 10 and AOD of 0.5 for an uncertain single-scattering albedo (SSA) of ±0.03
CALIOP Operational Method *Winker et al.* [2009]; *Young and Vaughan* [2009]	Vertically resolved aerosol backscatter and inferred extinction profile	Extinction to backscatter ratio and feature/layer detection scheme	Attenuated backscatter profile at 532 and 1 064 nm at 0.3 km scale	Vertical extinction profile, AOD at 532 and 1064 nm and at 0.3 and 5 km (level 2) scales	From *Winker et al.* [2009]: $0.05 + 0.40 \times AOD$,
CALIOP Depolarization Method *Hu et al.* [2007]	Change in the transmittance (DR) VIS/IR when absorbing aerosols overlay cloud	Cloud extinction-to-backscatter ratio at 532 nm and Rayleigh correction above cloud	Layer integrated attenuated backscatter and depolarization ratio at 532 nm	ACAOD at 532 nm	Depends on the integrated attenuated backscatter at 532 and its depolarization ratio.
CALIOP Color Ratio Method *Chand et al.* [2008]	Change in the VIS/IR transmittance when absorbing aerosols overlay cloud	Ångström Exponent (532–1064 nm) and color ratio (VIS/IR) of underlying cloud layer	Layer integrated attenuated backscatter and color ratio at 532 nm	ACAOD at 532 nm and Ångström exponent in the 532–1064 nm range	Depends on the integrated attenuated backscatter at 532 nm and 1064 nm and Ångström exponent
POLDER *Waquet et al.* [2009, 2013]	Creation of polarization at forward scattering angles. Reduction of the polarized signal in the cloudbow.	Six fine-mode spherical aerosol models with refractive index of 1.47–0.01i, one nonspherical-mineral dust model, and only one aerosol/cloud profile.	TOA polarized radiance at 670 and 865 nm at $6 \times 6\ km^2$ resolution (POLDER) and cloud droplets effective radius (MODIS)	AOD at 865 nm and Angström exponent. The AOD is converted at 500 nm using the retrieved Angström exponent.	Depends on AOD and microphysics. For an AOD of 0.2 (at 865 nm) : AOD error of 0.05 for a real refractive index uncertainty of +/−0.06 and error of 0.02 for an imaginary refractive index uncertainty of +/−0.01
OMI *Torres et al.* [2012]	Change in the near-UV reflectance and UV aerosol index (UVAI) when absorbing aerosols overlay cloud	Aerosol/cloud size distribution, aerosol spectral extinction and absorption, aerosol/cloud profiles, and surface albedo	TOA reflectance at 388 nm and measured UVAI at $13 \times 24\ km^2$ resolution	ACAOD and aerosol-corrected COD at 388 nm; converted to 500 nm based on model assumed spectral extinction	Depends on ACAOD and COD. Typically between −23 and 43% at COD of 10 and AOD of 0.5 for an uncertain SSA of ±0.03

ratio. Both the transmission methods require some screening criteria and independent calibration constants. The details of the DR and CR methods are given by *Hu et al.* [2007] and *Chand et al.* [2008], respectively.

2.4. POLDER

Aerosols above clouds generate an additional polarized signal at forward scattering angles and reduce the polarized signal of the cloudbow. The operational algorithm developed for the POLDER instrument takes advantage of these effects to retrieve the AOD above clouds and an aerosol model. The method consists of a comparison between the polarized radiance measured at 670 and 865 nm and precomputed polarized radiances using six spherical fine-mode and one coarse mode mineral dust aerosol models. The aerosol properties are first retrieved at a spatial resolution of $6 \times 6\ km^2$ (i.e., POLDER native resolution) and then aggregated at a resolution of $18 \times 18\ km^2$. The cloud properties retrieved from MODIS and POLDER were colocated to characterize the cloudy scenes. The algorithm is applied only to homogeneous cloudy pixels associated with optically thick liquid water clouds (COD > 3). More details about the various filters used to obtain a quality-assessed product and aerosol models can be found in the work of *Waquet et al.* [2013]. Table 1 summarizes the basic properties of different ACA techniques that are applied to the A-train sensors.

2.5. Colocation

Different sensors on the A-train satellites observe the same part of the Earth within a few minutes. The relative position of the A-train satellites (hence time difference) has gone through some changes since the inception of the constellation (http://atrain.nasa.gov/historical_graphics.php). The case studies examined in this paper belong to August 2006 and 2007, during which the time differences between Aqua and CALIPSO, CALIPSO and PARASOL, and PARASOL and Aura were about 1, 2, and 5 min, respectively. It is assumed that the cloud and aerosol systems do not change significantly during such short span. The spatial resolution of the A-train sensors however is different and therefore intercepts different coverage. While high-resolution

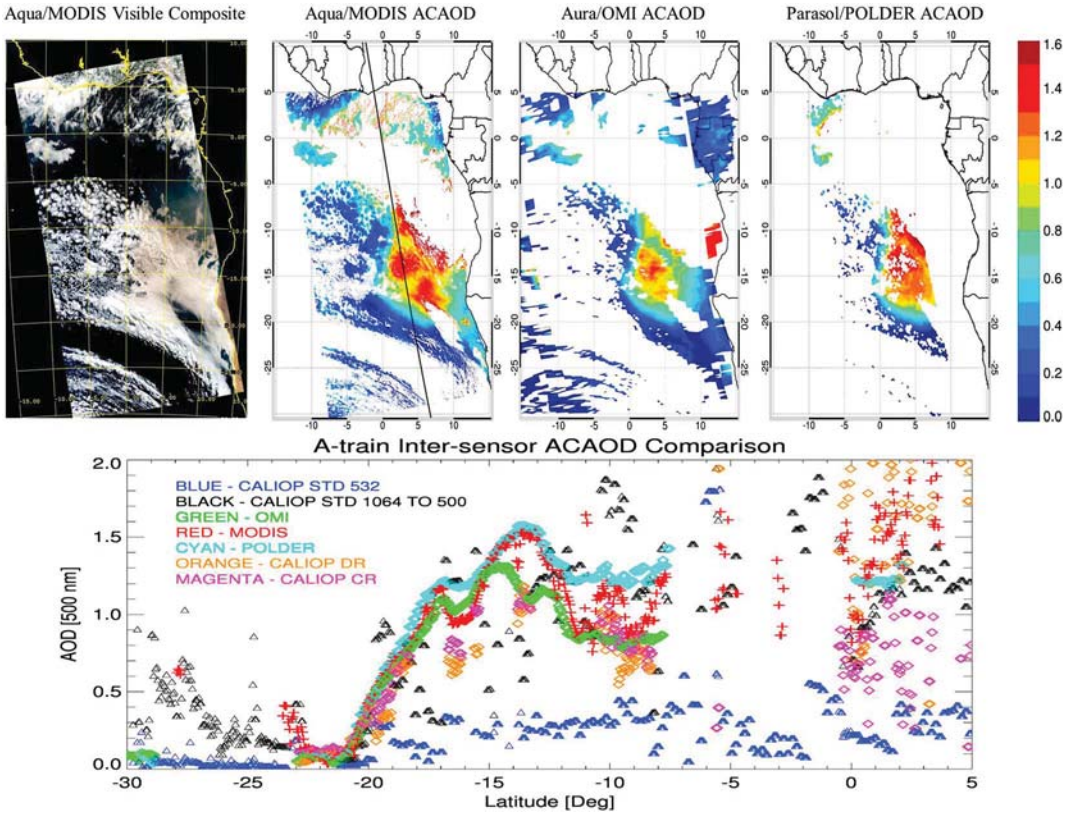

Figure 1. An above-cloud aerosol event observed over the southeast Atlantic Ocean on 13 August 2006. (top) The spatial plots of ACAOD retrieved from passive sensors are displayed. The CALIOP track is imposed on the MODIS plot. (bottom) A comparative plot of ACAOD along the CALIOP track.

sensors such as MODIS and CALIOP make measurements at subkilometer scales, POLDER on PARASOL platform intercept Earth with a footprint of size $6 \times 6\,km^2$ and OMI on Aura has even larger footprint of $13 \times 24\,km^2$. We consider the CALIOP along-track level 2 geolocation as a reference track for the intercomparison of ACAOD. In order to match with the 5 km averaged CALIOP retrievals, MODIS's 1 km ACAOD retrievals were also averaged to $5\,km^2$ grid box. Due to their coarser spatial resolutions, OMI and POLDER ACAOD retrievals were not averaged. We adopt the closest pixel approach (maximum distance ~5 km) to colocate passive sensors with the lidar retrievals.

3. Results

We have selected SEAO as a test bed to intercompare the different satellite retrievals. During dry season (July through September), the region-wide intense biomass burning over southern Africa emits huge amounts of carbonaceous particulate matter into the atmosphere, which, under the influence of prevailing westerly winds, is often advected over the boundary layer marine stratocumulus clouds. Two case study events of ACAOD are selected for the present analysis.

Figure 1 (top left) shows a true color RGB image made from two MODIS L1 5 min granules over SEAO on 13 August 2006. The rest three plots on top display the spatial distribution of ACAOD retrieved from Aura/MODIS, Aqua/OMI, and PARASOL/POLDER, respectively. All three passive sensors, in general, retrieve similar spatial pattern of ACAOD with maximum aerosol concentration off the western coast of southern Africa. Spatial coverage of ACAOD retrieved by three sensors is different. MODIS provides maximum retrieval availability followed by OMI and POLDER. Due to their coarser spatial resolution, OMI and POLDER algorithms

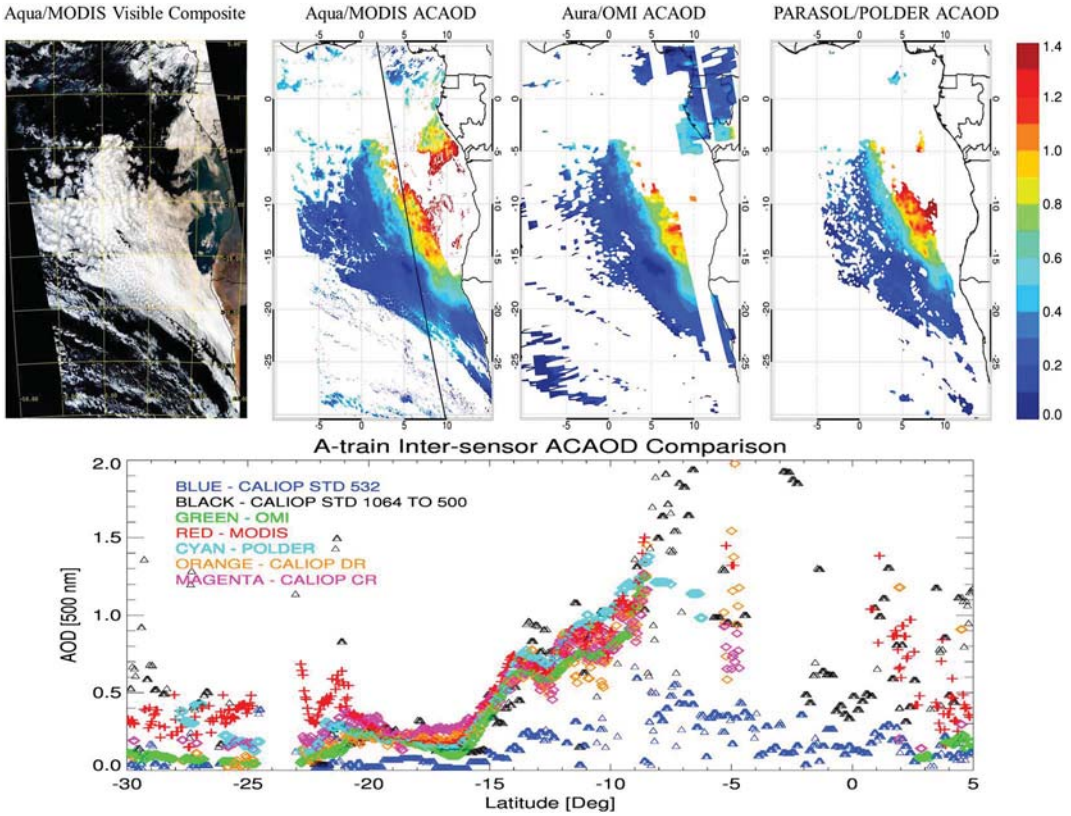

Figure 2. Same as in Figure 1 but for an above-cloud aerosol event observed by the A-train sensors on 2 August 2007.

reject pixels with partial cloud cover, whereas the finer pixel size of MODIS (250–500 m) can adequately capture small-scale clouds, thus yield more retrieval coverage.

Figure 1 (bottom) shows a comparative plot of ACAOD along the CALIOP track for the same case. All three passive sensors (MODIS, POLDER, and OMI) are found to be in close agreement (ΔACAOD ~ 0.1) between the latitude coverage 23°S to 15°S. Between 15°S and 12°S, MODIS tends to retrieve higher AOD than those of OMI and POLDER. Throughout the spatial extent of this event (30°S to 5°S), CALIOP's standard 532 nm retrievals are lower by a factor as large as 5 or even more relative to the passive sensors. However, CALIOP standard 1064 nm retrieval converted to 500 nm using POLDER's Ångström exponent brings lidar retrieval closer to the passive sensors.

Largest discrepancy between all sensors is seen between the equator and 5°N, where the true color image shows presence of small-scale broken clouds. Over this area, MODIS and CALIOP-based DR method retrieve very large values of AOD (~2.0) followed by POLDER and CALIOP 1064 nm retrieving AOD of about 1.3; CALIOP-based CR method derives a range of values between 0.5 and 1, and finally CALIOP standard 532 nm AOD (~0.3–0.4) are falling the lowest in the comparison. A few retrievals from CALIOP and MODIS around latitude 6°S correspond to thin clouds. POLDER and OMI do not attempt retrieval over this region due to partial cloud coverage in their bigger footprints. However, owing to have higher resolution, both CALIOP and MODIS are able to detect the presence of aerosols above cloud over small-scale cloud fields. The magnitudes of retrieved ACAOD are however significantly different.

The results for the second case study, 2 August 2007, are shown in Figure 2. Similar to the previous case, all three passive sensors retrieve consistent spatial distribution of ACAOD with variable spatial coverage. The ACAOD intercomparison plot in Figure 2 (bottom) shows close agreement (ΔACAOD ~ 0.1–0.2)) among all the sensors except CALIOP 532 nm retrieval between latitude 23°S and 9°S. A few retrievals from CALIOP and MODIS around latitude 5°S correspond to very thin and shallow clouds, where both sensors retrieve significantly different AOD. Also, the discrepancy between all sensors is large over the broken cloud region between the equator and 5°N.

4. Discussion and Conclusion

The accuracy of the ACAOD retrieval from each sensor depends on several factors, which are briefly discussed here. All methods compared here assume that the sensor footprint is fully overcast. This requirement can be assured by the higher spatial resolution sensor MODIS and CALIOP. Coarser resolution sensors OMI and POLDER intercept larger area at surface and therefore require robust cloud mask. The impact of sensor resolution is reflected in the different spatial coverage of retrieval in Figures 1 and 2. Moreover, the air mass and thus AOD captured by different sensors directly depends on the pixel size and (in)homogeneity of aerosol loading. This can be a source of disagreement between different sensors. The particle microphysics and cloud droplet distribution assumed in the aerosol model can be an important source of uncertainty in the ACAOD retrieval. For instance, the color ratio algorithm applied to MODIS and OMI requires assuming the aerosol and cloud size distribution, and more importantly the imaginary part of the refractive index or single-scattering albedo (ω). The aerosol models used in the CR algorithms are essentially derived from the AERONET inversions, which themselves carry retrieval uncertainty; for instance, ω is expected to be accurate within ± 0.03. An uncertain ω beyond 0.03 can result in an ACAOD retrieval error of about 50% or larger [*Torres et al*., 2012; *Jethva et al*., 2013].

The retrieval accuracy for the operational POLDER algorithm mainly depends on the assumptions made for the aerosol microphysical properties. Polarization measurements at 670 and 865 nm are primarily sensitive to the optical thickness of scattering. The method retrieves the total (scattering and absorbing) AOD by assuming a constant value of 0.01 for the imaginary part of the complex refractive index. A relative AOD error of 10% at 865 nm is expected for an imaginary refractive index uncertainty of 0.01. The assumption made for the real refractive index also impacts the AOD retrievals (see Table 1). The good quantitative agreement observed between the POLDER, OMI, and MODIS AODs, estimated at 500 nm, suggests that the Ångström exponent retrieved by POLDER is also well estimated. The POLDER algorithm is only applied to homogeneous cloudy pixels associated with a cloud fraction of 100% and a COD larger than 3, thus ensuring the accuracy of the retrieved AOD.

The CALIOP-based CR method assumes the aerosol Ångström exponent and the calibration constant or color ratio for unobstructed cloud targets. For instance, an error of -0.5 in Ångström exponent can cause about 18% underestimation in CR-based ACAOD relative to that of DR result. Actual variations in these parameters, if not accounted for in the inversion, are the possible sources of uncertainty. The accuracy of DR method relies on the accuracy of the lidar calibration and assumed layer-integrated attenuated backscatter (532 nm) for unobstructed clouds.

While the CALIOP standard 532 nm AOD is found to be significantly lower by a factor of 4 to 6 relative to passive retrievals, the 1064 nm ACAOD when converted to the 500 nm using the POLDER-retrieved Ångström exponent (black triangles in Figures 1 and 2) shows a closer agreement with retrievals from passive sensors. An analogous result has also been observed by *Omar et al*. [2013], where CALIOP standard 532 nm AOD retrievals were found to underestimate AERONET measurements by about 40–50%, while its 1064 nm retrievals did not show any obvious underestimation and were in better agreement with those of AERONET. *Kacenelenbogen et al*. [2011] also noted that CALIOP is underpredicting cloud-free AOD (532 nm) of a biomass burning aerosol plume by a factor of 2 compared to the coincident high spectral resolution lidar, ground-based, and other satellite measurements for a case study over the mid-Atlantic region in the U.S. For an optically thick absorbing aerosol layer, the two-way lidar signal undergoes a strong attenuation which can lead to weak or even loss of signal particularly from the lower layers. A possible explanation of the reduced signal in the presence of carbonaceous particles is the effect of aerosol absorption that, at the typically large optical depth values of smoke layers, would yield large aerosol absorption optical depths that significantly reduce the number of backscattered photons [*Torres et al*., 2013]. This effect would be more pronounced at shorter wavelengths (owing to the stronger extinction: scattering and absorption) than at longer wavelengths (1064 nm). As a result, the CALIOP 532 nm signal detects only a fraction of the absorbing layers, whereas the 1064 nm measurements observe the entire aerosol column above an opaque surface (refer to the curtain images of CALIOP backscatter for the present two case studies at http://www.calipso.larc.nasa.gov/products/lidar/browse_images/). Furthermore, misclassification of aerosol types and subsequent use of inappropriate lidar ratio can be an additional source of uncertainty in the CALIOP standard retrieval.

A detailed analysis on the attribution of the differences to various sources of uncertainties for the present case studies is currently out of the scope of this paper due to space limitation. The sensitivity analysis of the

ACAOD retrievals is reported in the lead algorithm papers referenced in the Introduction. Due to the scarcity of direct measurements of ACAOD, it is hard to quantify the actual uncertainty in each of the present retrieval methods. The suborbital direct measurements of aerosols above cloud are strongly needed over the regions of SEAO (smoke above cloud), tropical Atlantic Ocean (smoke and dust above cloud), and Southeast Asia (smoke and pollution above cloud), where the elevated layers of absorbing aerosols over cloud are often observed from satellites.

Given that each ACAOD method is designed independently and relies on different types of measurements from different sensors, an overall close agreement between them over the homogeneous cloud fields is an encouraging result. Such intercomparison should be further extended to multiple events, regions, and spatial/temporal scales for the comprehensive evaluation. It is expected that the ACAOD research methods will be applied to produce operational products in the coming years, which in conjunction with the standard cloud-free aerosol products will provide us with an unprecedented all-sky aerosol distribution from space. This can substantially enhance our knowledge on how aerosols affect the cloud radiative forcing and microphysical properties, and aerosol transport.

Acknowledgments

We acknowledge the support of all NASA data centers, i.e., LAADS, ASDC, and GES-DISC for the online availability of various satellite products used in this analysis. We thank Ali Omar (NASA Langley) for the useful discussion on CALIOP operational product. The research work of F. Waquet has been supported by the Programme National de Télédétection Spatiale (PNTS, http://www.insu.cnrs.fr/actions-sur-projets/pnts-programme-national-de-teledetection-spatiale), grant PNTS-2013-10.

The Editor thanks an anonymous reviewer for assisting in the evaluation of this paper.

References

Chand, D., T. L. Anderson, R. Wood, R. J. Charlson, Y. Hu, Z. Liu, and M. Vaughan (2008), Quantifying above-cloud aerosol using spaceborne lidar for improved understanding of cloudy-sky direct climate forcing, *J. Geophys. Res.*, *113*, D13206, doi:10.1029/2007JD009433.

Chand, D., R. Wood, T. L. Anderson, S. K. Satheesh, and R. J. Charlson (2009), Satellite-derived direct radiative effect of aerosols dependent on cloud cover, *Nat. Geosci.*, *2*, 181–184, doi:10.1038/ngeo437.

Haywood, J. M., S. R. Osborne, and S. J. Abel (2004), The effect of overlying absorbing aerosol layers on remote sensing retrievals of cloud effective radius and cloud optical depth, *Q. J. R. Meteorol. Soc.*, *130*, 779–800, doi:10.1256/qj.03.100.

Hu, Y., M. Vaughan, Z. Liu, K. Powell, and S. Rodier (2007), Retrieving optical depths and lidar ratios for transparent layers above opaque water clouds from CALIPSO lidar measurements, *IEEE Geosci. Remote Sens. Lett.*, *4*(4), 523–526, doi:10.1109/LGRS.2007.901085.

Jethva, H., O. Torres, L. A. Remer, and P. K. Bhartia (2013), A color ratio method for simultaneous retrieval of aerosol and cloud optical thickness of above-cloud absorbing aerosols from passive sensors: Application to MODIS measurements, *IEEE Trans. Geosci. Remote Sens.*, *51*(7), 3862–3870, doi:10.1109/TGRS.2012.2230008.

Kacenelenbogen, M., M. A. Vaughan, J. Redemann, R. M. Hoff, R. R. Rogers, R. A. Ferrare, P. B. Russell, C. A. Hostetler, J. W. Hair, and B. N. Holben (2011), An accuracy assessment of the CALIOP/CALIPSO version 2/version 3 daytime aerosol extinction product based on a detailed multi-sensor, multi-platform case study, *Atmos. Chem. Phys.*, *11*, 3981–4000, doi:10.5194/acp-11-3981-2011.

Keil, A., and J. M. Haywood (2003), Solar radiative forcing by biomass burning aerosol particles during SAFARI 2000: A case study based on measured aerosol and cloud properties, *J. Geophys. Res.*, *108*(D13), 8467, doi:10.1029/2002JD002315.

Omar, A. H., D. M. Winker, J. L. Tackett, D. M. Giles, J. Kar, Z. Liu, M. A. Vaughan, K. A. Powell, and C. R. Trepte (2013), CALIOP and AERONET aerosol optical depth comparisons: One size fits none, *J. Geophys. Res. Atmos.*, *118*, 4748–4766, doi:10.1002/jgrd.50330.

Torres, O., H. Jethva, and P. K. Bhartia (2012), Retrieval of aerosol optical depth above clouds from OMI observations: Sensitivity analysis and case studies, *J. Atmos. Sci.*, *69*, 1037–1053, doi:10.1175/JAS-D-11-0130.1.

Torres, O., C. Ahn, and Z. Chen (2013), Improvements to the OMI near UV aerosol algorithm using A-train CALIOP and AIRS observations, *Atmos. Meas. Technol.*, *6*, 3257–3270, doi:10.5194/amt-6-3257-2013.

Waquet, F., J. Riedi, L. C. Labonnote, P. Goloub, B. Cairns, J.-L. Deuzé, and D. Tanré (2009), Aerosol remote sensing over clouds using A-train observations, *J. Atmos. Sci.*, *66*, 2468–2480, doi:10.1175/2009JAS3026.1.

Waquet, F., et al. (2013), Retrieval of aerosol microphysical and optical properties above liquid clouds from POLDER/PARASOL polarization measurements, *Atmos. Meas. Technol.*, *6*, 991–1016, doi:10.5194/amt-6-991-2013.

Winker, D. M., M. A. Vaughan, A. Omar, Y. Hu, K. A. Powell, Z. Liu, W. H. Hunt, and S. A. Young (2009), Overview of the CALIPSO mission and CALIOP data processing algorithms, *J. Atmos. Oceanic Technol.*, *26*(11), 2310–2323, doi:10.1175/2009JTECHA1281.1.

Young, S. A., and M. A. Vaughan (2009), The retrieval of profiles of particulate extinction from Cloud-Aerosol Lidar Infrared Pathfinder Satellite Observations (CALIPSO) data: Algorithm description, *J. Atmos. Oceanic Technol.*, *26*, 1105–1119, doi:10.1175/2008JTECHA1221.1.